



**Titre:** Sinterability of macrocrystalline and cryptocrystalline magnesite to refractory magnesia  
Title:

**Auteurs:** Zongqi Guo, Ying Ma, & Michel Rigaud  
Authors:

**Date:** 2020

**Type:** Article de revue / Article

**Référence:** Guo, Z., Ma, Y., & Rigaud, M. (2020). Sinterability of macrocrystalline and cryptocrystalline magnesite to refractory magnesia. International Journal of Ceramic Engineering & Science, 2(6), 303-309.  
Citation: <https://doi.org/10.1002/ces2.10068>

 **Document en libre accès dans PolyPublie**  
Open Access document in PolyPublie

**URL de PolyPublie:** <https://publications.polymtl.ca/10637/>  
PolyPublie URL:

**Version:** Version officielle de l'éditeur / Published version  
Révisé par les pairs / Refereed

**Conditions d'utilisation:** CC BY  
Terms of Use:

 **Document publié chez l'éditeur officiel**  
Document issued by the official publisher

**Titre de la revue:** International Journal of Ceramic Engineering & Science (vol. 2, no. 6)  
Journal Title:

**Maison d'édition:** Wiley  
Publisher:

**URL officiel:** <https://doi.org/10.1002/ces2.10068>  
Official URL:

**Mention légale:** This is an open access article under the terms of the Creative Commons Attribution License, which permits use, distribution and reproduction in any medium, provided the original work is properly cited. © 2020 The Authors. International Journal of Ceramic Engineering & Science published by Wiley Periodicals LLC on behalf of American Ceramic Society  
Legal notice:

## ORIGINAL ARTICLE

# Sinterability of macrocrystalline and cryptocrystalline magnesite to refractory magnesia

Zongqi Guo<sup>1</sup>  | Ying Ma<sup>2</sup> | Michel Rigaud<sup>3</sup><sup>1</sup>Yingkou Jindai Technologies, Jiachen Group, Yingkou, China<sup>2</sup>RHI Magnesita (Dalian) Co., Ltd., Dalian, China<sup>3</sup>Ecole Polytechnique, University of Montreal, Montreal, QC, Canada**Correspondence**

Zongqi Guo, Yingkou Jindai Technologies, Jiachen Group, China.

Email: zguo.lemonde@outlook.com

**Abstract**

The purpose of this paper is to present the results of an investigation aiming at obtaining high quality sintered magnesia from two well-known Chinese magnesite. Two types of natural magnesite have been considered, one macrocrystalline, from Liaoning, with the grain size of 60–100  $\mu\text{m}$  and one cryptocrystalline, from Tibet, with 2–4  $\mu\text{m}$  grains. Calcining characteristics to transform the two magnesite to caustic magnesia have been studied at first. Subsequently, the calcining-sintering characteristics using a two- and a three-step process for both raw materials at different temperatures have been determined. A DTA–TGA study reveals that the minimum endothermic peak during the calcining step differs by 28°C (624 vs 652°C between the crypto- and macrocrystalline magnesite). It has also been observed that by using a two-step sintering process, it is possible to obtain a magnesia with a bulk density of 3.26 and 3.14  $\text{g}/\text{cm}^3$ , respectively, for cryptocrystalline and macrocrystalline, while with a three-step process, it is possible to reach a bulk density of 3.48  $\text{g}/\text{cm}^3$ , even at a temperature <1750°C.

**KEYWORDS**

densification, hydration, magnesia, microstructure, sinter/sintering

## 1 | INTRODUCTION

There are two major sources to produce sintered refractory magnesia over the world. One is to concentrate  $\text{Mg}^{2+}$  from seawater or natural brine and to obtain the sintered dense magnesia at normal temperature of 1600–1700°C after calcining the precipitated magnesium hydroxide.<sup>1</sup> The other is to calcine natural magnesite ( $\text{MgCO}_3$ ) and to sinter the compacts of caustic calcined magnesia at extremely high temperature of 1900–2100°C, to obtain top-grade quality grains with more than 98%  $\text{MgO}$  in purity, 3.45  $\text{g}/\text{cm}^3$  and higher in bulk density, and with large grains crystals containing few pores, low boron oxide ( $\text{B}_2\text{O}_3 < 0.05\%$ ) and the correct  $\text{CaO}/\text{SiO}_2$  molar ratio.<sup>2</sup>

During the last three decades, the sintered natural magnesia, from Liaoning area, has been one of the prevailing raw materials for worldwide refractory manufacturers. It is called as dead burnt magnesia (DBM97) with the bulk density of 3.26–3.30  $\text{g}/\text{cm}^3$ . With the increasing demand for higher purity-grade magnesia, it became necessary to make use of reverse flotation to remove  $\text{SiO}_2$  carrying portion and to upgrade caustic magnesia to 98%  $\text{MgO}$ , calcined by either multi-hearth furnace or suspension calciner.

Recently, a magnesite reserve of ~200 million tons in Riwoqe county, Tibet, has been considered.<sup>3,4</sup> In this investigation, both types of magnesite, from Liaoning and Tibet, are studied to compare their main characteristics after calcining and sintering in a

This is an open access article under the terms of the Creative Commons Attribution License, which permits use, distribution and reproduction in any medium, provided the original work is properly cited.

© 2020 The Authors. *International Journal of Ceramic Engineering & Science* published by Wiley Periodicals LLC on behalf of American Ceramic Society

two-step process and in a three-step process of calcining, hydrating, recalcining and sintering at various temperatures.

## 2 | EXPERIMENTAL PROCEDURE

The fracture morphology of both magnesite ores is shown in Figure 1. The ranges of grain sizes have been obtained using a ZEISS/EVO18 scanning electron microscope. The floated magnesite containing grains of 60–100  $\mu\text{m}$  comes from the Haicheng-Dashiqiao district in Liaoning, and the Tibetan magnesite, with 2–4  $\mu\text{m}$  grains, is located in a 3800 m-altitude deposit of Riwoqe County, Tibet. Generally, magnesite ore shows the dependent structural crystal, without pores and defects after perfect growth.

The purification was made to remove silicate-carrying portion by the reverse floatation, from crushed and milled magnesite, and so the floated macrocrystalline magnesite is received as powder. The cryptocrystalline magnesite lumps are also crushed and milled prior to various tests.

The chemical analyses of both magnesites have been determined by X-Ray Fluorescence, using a Bruker AXS/S4 PIONEER spectrometer and presented in Table 1.

The MgO content in both raw materials is over 98%, with almost the same impurity levels of  $\text{SiO}_2$ ,  $\text{Al}_2\text{O}_3$ , and CaO. But

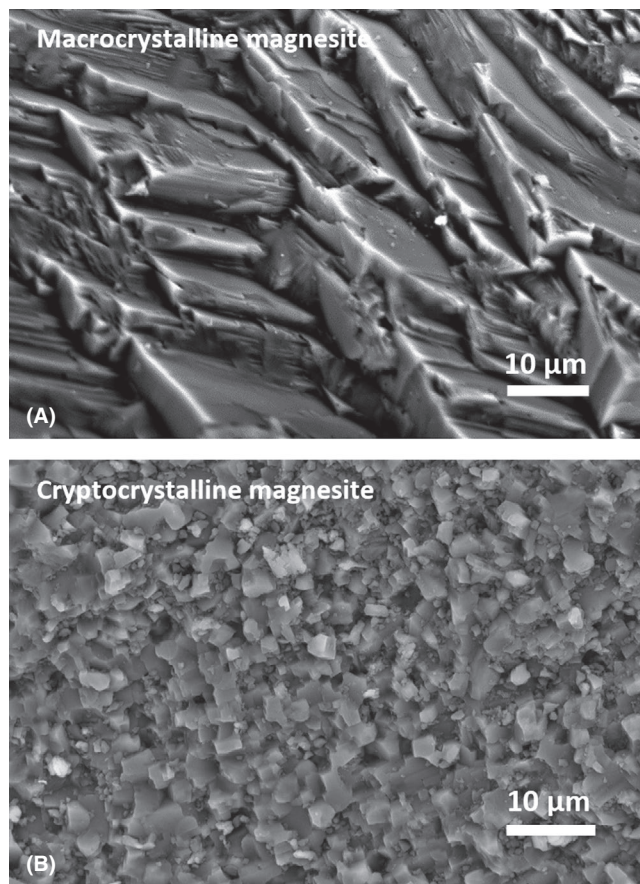


**FIGURE 1** Fracture morphology of macrocrystalline and cryptocrystalline magnesite

the trace content of  $\text{Fe}_2\text{O}_3$  is significantly lower in the Tibetan magnesite than about 0.6% in Liaoning floated magnesite.

The bulk density has been measured using mercury as an immersing media, according to GB/T 2999-2002 procedure. The decomposition temperature of 200-mesh magnesite powder is determined by thermo gravimetric analyzer (NETZSCH/DSC200F3). The particle size is measured by laser analyzer (Cilas/920L). Magnesium hydroxide is identified by X-ray diffraction (XRD) patterns (Rigaku/D-MAX 3B). Microstructural observation and the measurement of periclase crystal sizes are made by reflection optical microscopy (Nikon/Eclipse L150A), following the linear intercept procedure of ASTM E112-96(2006). The periclase crystal size is measured on the polishing section made of 60 grains of 3–5 mm in size, to match/record certain grids under microscope and then to calculate the average crystal size.

The activity of caustic calcined magnesia is tested by reacting with citric acid. The solution used at  $\text{pH} = 2.5$  is obtained from the diluted citric acid of  $\text{pH} = 1.95$  by adding distilled water. The caustic calcined magnesia of 2.0 g is put into 200 ml beaker, which is under magnetic mixer with the consistent temperature of  $24^\circ\text{C}$ . Turn on the mixer to 500 rpm and the second chronograph, and insert pH test strips in the solution immediately after 100 ml solution of citric acid is poured into the beaker. When pH value reaches 7.0, the number of the second is recorded by a counter to indicate the finished acid-base reaction. The activity is reflected by the second counting number of the reaction time between the caustic calcined magnesia and citric acid solution.

## 3 | RESULTS AND DISCUSSION

### 3.1 | The DTA-TGA variation

Differential thermal analysis (DTA) and thermo gravimetric analysis (TGA) patterns are shown in Figure 2 for

**TABLE 1** The chemical analyses of Tibetan and Liaoning magnesite

Deposit origin	Tibet	Liaoning
Magnesite type	Cryptocrystalline	Macrocrystalline
Magnesite status received	Raw ore lump	Floated powder
Loss on ignition ( $1050^\circ\text{C}$ )	50.81	51.68
Determination by XRF	(After loss on ignition)	
$\text{SiO}_2$	0.23	0.25
CaO	0.96	0.94
$\text{Fe}_2\text{O}_3$	0.03	0.59
$\text{Al}_2\text{O}_3$	0.02	0.04
MgO	98.75	98.18

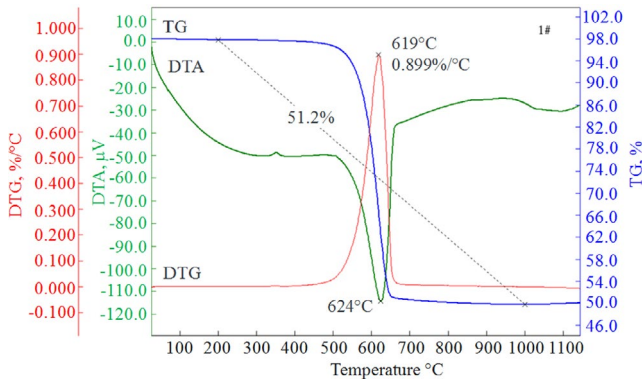
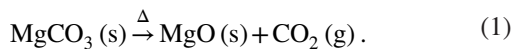


**FIGURE 2** Differential thermal analysis (DTA) and thermo gravimetric analysis (TGA) patterns of cryptocrystalline magnesite

cryptocrystalline magnesite and in Figure 3 for macrocrystalline magnesite.

Cryptocrystalline magnesite starts to decompose at 510°C and finishes at 690°C, which is an endothermic reaction. The decomposition reaction takes place most dramatically at 624°C, which corresponds to the endothermic peak in Figure 2. Macrocrystalline magnesite decomposes at the temperatures between 512 and 712°C, with the endothermic peak at 652°C in Figure 3. Two types of magnesite have very similar characteristics of DTA–TGA variations, but the temperature of endothermic peak for cryptocrystalline magnesite is 28°C lower than that for macrocrystalline magnesite.

Thermal decomposition of magnesite is a solid-gas endothermic reaction to generate a solid phase MgO and a gaseous phase CO<sub>2</sub>, in the following equation.



The weight loss ratio is 51.2% for cryptocrystalline magnesite and 53.8% for macrocrystalline magnesite. Comparing with theoretical value of magnesite decomposition of 52.19% calculated from the Equation (1), the thermal decomposition

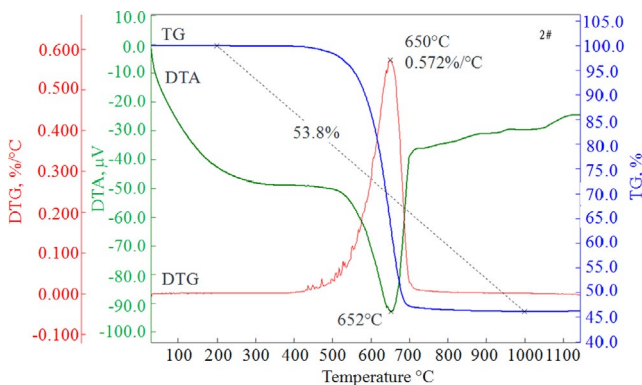


**FIGURE 3** Differential thermal analysis (DTA) and thermo gravimetric analysis (TGA) patterns of macrocrystalline magnesite

is completed, generally. There is only one step of weight loss that is corresponding to one endothermic peak in both TG curves, which suggests that magnesite decomposition takes place in a one-step reaction.

### 3.2 | Influence of calcining temperatures on the activity of caustic magnesia

Both types of magnesite have been calcined at various temperatures between 600 and 1300°C, for 2 hours, respectively. After milling to  $D_{50} = 10\mu\text{m}$ , their activities have been determined according to the reaction time of calcined caustic magnesia (CCM) with citric acid, which is shown in Figure 4.

Since high activity of CCM results in short reaction time, the highest activity occurs at calcining temperature of 700°C for cryptocrystalline magnesite and 800°C for macrocrystalline magnesite. There is tardy acidic reaction of CCM from cryptocrystalline magnesite fired at the temperature lower than 650°C. The fast reaction occurs over 650°C, until 1300°C. However, CCM from macrocrystalline magnesite is inert to react with citric acid at the temperature lower than 700°C and higher than 1000°C. It is important to control calcining temperatures within the range between 750 and 900°C. Additionally, the activity is higher if CCM is ground to finer powder and the activity of CCM becomes important to enhance sinterability of CCM compacts.

Microstructural observations indicate decomposition reaction occurs from outer layer to inside, along cleavage plane of magnesite crystalline and with more cracks within grains. Rao's study proved that the particles of calcined magnesia powder are alike, somewhat smaller than those

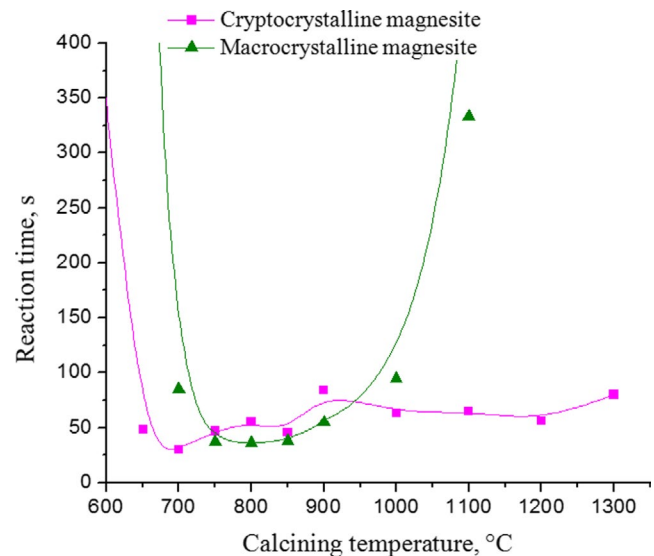


**FIGURE 4** Reaction time of caustic magnesia calcined at various temperatures, with citric acid



of flotation-beneficiated magnesite particles in size, but their particle shapes look similarly rhombohedral.<sup>5</sup> It suggests the magnesite particles, after the liberation of carbon dioxide, remain the original shape to be the hard pseudomorphic particles or aggregates. Further calcination makes magnesia crystals get sintered within the pseudomorphic particles.<sup>6</sup> In the first phase, the crystals get rapid growth and the pseudomorphic aggregates get shrinkages to certain extent. Then, it is a sintering process governed by evaporation-condensation or surface diffusion mechanism. The growth of crystals is rapid at the beginning, but reduces to low speed. There is no significant shrinkage and change of the pseudomorphic aggregates, where the pores become large. Finally, the diffusion on crystal boundary starts working and the pseudomorphic aggregates shrink again. In the case of block magnesite ore, the volume of pseudomorphic aggregates contract, resulting in the decrease of coordination numbers and the specific surface area and sintering densification is impeded, showing slow densification process.<sup>7</sup> Additionally because of high strength, the aggregates are hardly to be disrupted under the ordinary compacting pressure.

Because of the pseudomorphic aggregates, it is not possible to sinter directly magnesia from magnesite in China, to an acceptable level of bulk density. The common industrial practice is to calcine magnesite firstly, to grind and compact, and finally to sinter at very high temperature.

### 3.3 | Sintered results, using both magnesites in a two-step process

Such a two-step process sintering is schematically summarized in Figure 5. It is proved that there is no significant influence of original size of magnesite ore (either small lump or powder) on CCM activity because the calcining process

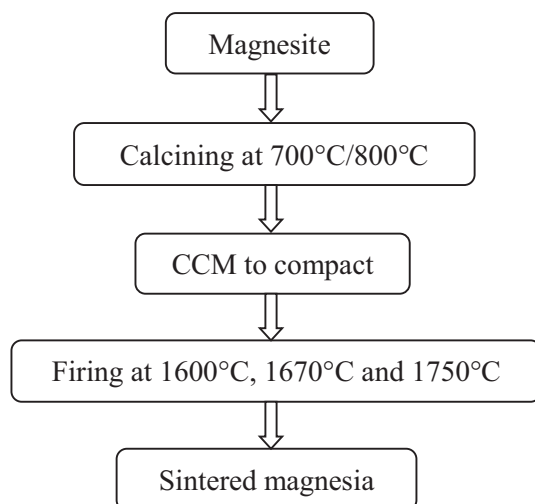


FIGURE 5 Two-step process sintering

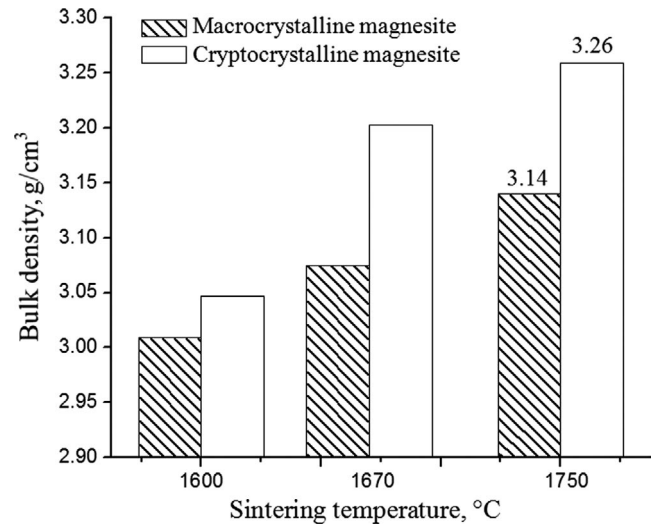


FIGURE 6 Bulk density as a function of sintering temperature

is driven by the decomposition of magnesite to release most portion of  $\text{CO}_2$ .

Macrocrystalline magnesite has been calcined at  $800^\circ\text{C}$  and cryptocrystalline magnesite at  $700^\circ\text{C}$  for 2 hours. After being crushed and milled for 24 hours to have the particle size of  $D_{50} = 10\mu\text{m}$ , both types of CCM are pressed under 100 MPa to prepare compacts of  $25 \times 25 \times 125$  mm bars. After being dried at  $120^\circ\text{C}$  for 12 hours, the compacts are fired at 1600, 1670, and  $1750^\circ\text{C}$  for 6 hours, respectively, being available burning temperatures in tunnel kilns.

As expected, the bulk density of the compacts after sintering increases significantly with temperatures, as shown in Figure 6. It reaches a maximum of only 3.14 and  $3.26\text{ g/cm}^3$  at  $1750^\circ\text{C}$  for macro- and cryptocrystalline samples, respectively. The periclase crystal sizes follow the same trend.

### 3.4 | Sintered results, using both magnesites, in a three-step process

The three-step process sintering is schematically illustrated in Figure 7.

After same calcination in Section 3.3, the calcined magnesia is ground with water for 24 hours. The resulting solution is heated at  $80\text{--}90^\circ\text{C}$  for 3 hours to make magnesia hydrated and dried at  $200^\circ\text{C}$  for 12 hours. It is then ground again for 5–6 hours to obtain brucite  $\text{Mg}(\text{OH})_2$  powder, with  $D_{50} = 4.43\mu\text{m}$  for the floated magnesia and  $D_{50} = 4.06\mu\text{m}$  for Tibetan magnesia. Both types of brucite  $\text{Mg}(\text{OH})_2$  powder are calcined at 500, 600, 700, 800, 900, and  $1000^\circ\text{C}$  for 1 hour, respectively, and then milled to active CCM powder ( $D_{50} = \sim 12\mu\text{m}$ ). The active  $\text{MgO}$  powder is pressed under the pressure of 180 MPa to make the cylinders of  $\phi 36$  mm in diameter and 50 mm in height. After dried at  $110^\circ\text{C}$ ,

the cylinders are fired at 1670 and 1750°C for 6 hours in tunnel kiln.

The XRD patterns for the two respective hydrated powders obtained prior to the second calcining step are shown in Figure 8, where the hydration degrees of only most active CCM are determined after macrocrystalline magnesite is calcined at 800°C and cryptocrystalline magnesite at 700°C. It is possible to acquire a content of about 89% brucite  $Mg(OH)_2$  and to remain ~11% periclase  $MgO$  from cryptocrystalline CCM against ~95% and ~5% from macrocrystalline CCM.

After re-calcination and sintering, the bulk density of the sintered magnesia obtained after sintering at either 1670 or 1750°C does vary with the recalcining temperature variations, as clearly shown in Figure 9.

All those results show the potential benefit to use a 3-step process rather than 2-step process, in other words, to sinter the calcining caustic magnesia derived from a transformed  $Mg(OH)_2$  mix rather than directly from the magnesite source, in order to obtain sintered magnesia with a bulk density of  $3.48\text{ g/cm}^3$ . Such results are in line with previous studies,

confirming the observations made by Ref [8–10], that is either first to grind CCM obtained from  $Mg(OH)_2$  rather than  $MgCO_3$ , then to produce higher bulk density after sintering

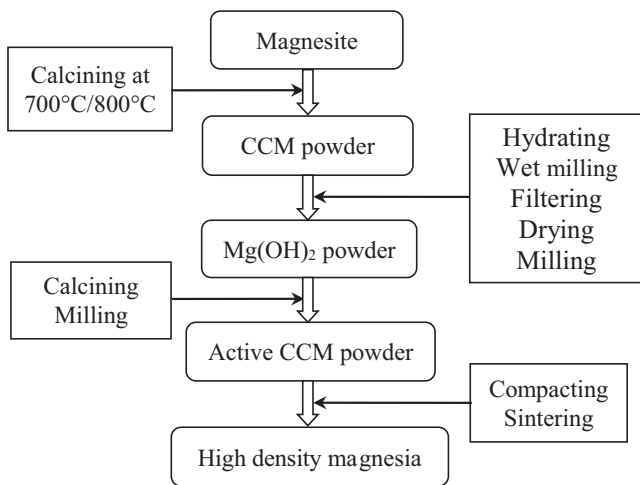


**FIGURE 7** Three-step process sintering

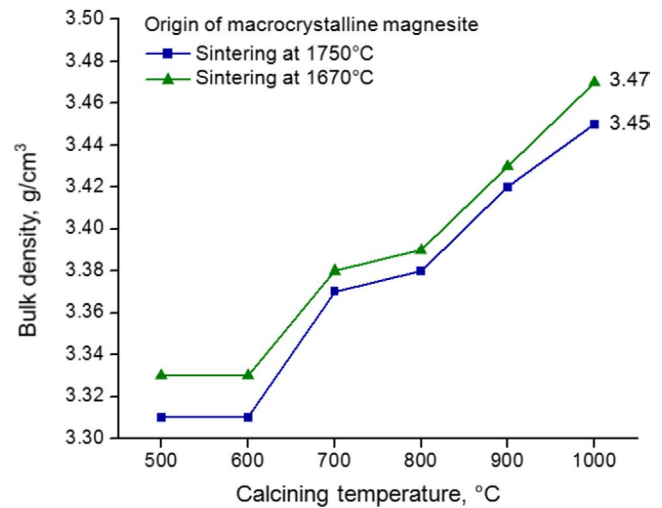
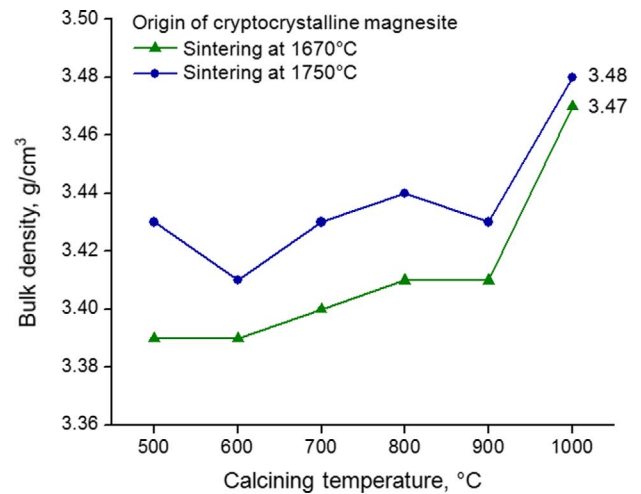


**FIGURE 9** Bulk density after sintering at either 1670 or 1750°C, as a function of the calcining temperature to obtain an active calcined caustic magnesia powder

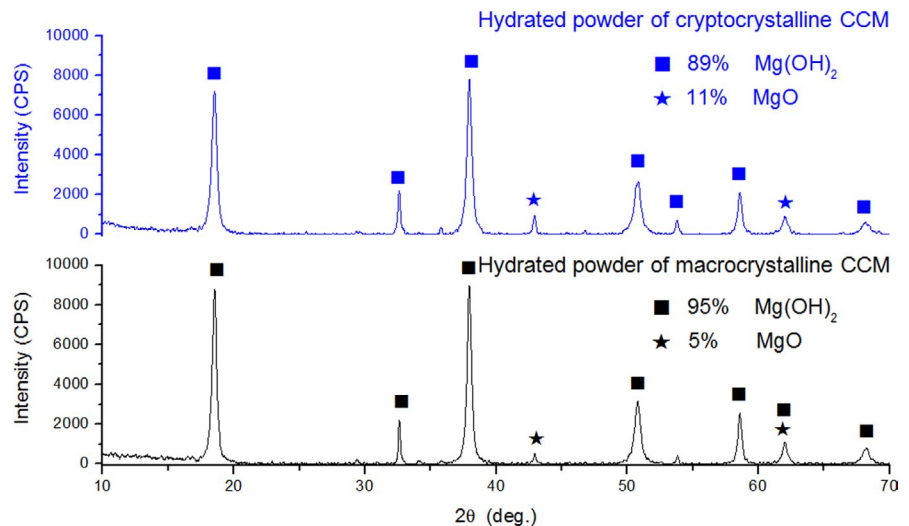


**FIGURE 8** XRD patterns of hydrated powders

Magnesite type and sintering temperature		Calcining temperature of Mg(OH) <sub>2</sub> powder, °C					
		500	600	700	800	900	1000
Macrocrystalline	1670°C	58	63	64	64	75	78
	1750°C	61	67	73	80	85	98
Cryptocrystalline	1670°C	88	92	94	96	106	115
	1750°C	92	94	105	107	110	117

**TABLE 2** Average crystal size of three-step sintered magnesia, μm

in the range of 1670 to 1750°C. Yu<sup>11</sup> found that the H<sub>2</sub>O involved during the decomposition of magnesium hydroxide was partially dissolved in MgO to generate many divacancies. It could be understood that no CO<sub>3</sub><sup>2-</sup> group residuum confinement and the dissolved H<sub>2</sub>O are very helpful to sintering in CCM of magnesium hydroxide.

Combined with the average crystal sizes listed in Table 2, it is clear to see that higher calcining temperatures are beneficial to crystal growth and sintering densification, particularly for cryptocrystalline magnesite. In both cases of cryptocrystalline and macrocrystalline magnesite, it is essential to calcine magnesium hydroxide at 1000°C to densify sintered magnesia over 3.45 g/cm<sup>3</sup>, which can be achieved either at 1670 C or 1750°C. Whatever the calcining temperature is, the better sintering temperature is 1670°C for macrocrystalline magnesite, whereas it is 1750°C for cryptocrystalline magnesite. It is very valuable to sinter magnesia at relatively low temperatures and with large temperature range for industrial process. Again by three-step sintering process, it is proven that it is more susceptible to sinter cryptocrystalline magnesite.

After calcining, hydrating, recalcining, and sintering, microstructures of high-purity, dense magnesia are shown in Figure 10. The periclase crystals are well grown, showing approximately hexagonal shapes. There are lots of small pores, particularly along the boundary of periclase crystals, in 1670°C sintered magnesia of macrocrystalline magnesite (Figure 10A). They become larger after sintered at 1750°C. The pores and defects are much smaller and less in sintered magnesia of cryptocrystalline magnesite (Figure 10B). The formation of interstitial phases depends on CaO/SiO<sub>2</sub> ratio along the route from 2MgO·SiO<sub>2</sub> to 2CaO·SiO<sub>2</sub> in the MgO–CaO–SiO<sub>2</sub> system. In the sintered magnesia with the high purity of >98% MgO and the high density of >3.45 g/cm<sup>3</sup>, the CaO/SiO<sub>2</sub> ratio, that is much larger than 2.2, must result in the formation of dicalcium silicate as the interstitial phase, which is difficult to be detected in fine boundary shown in Figure 10.

## 4 | CONCLUSIONS

1. Based on the same grain size of the powder and same amount used in the DTA-TGA tests, the cryptocrystalline magnesite starts decomposition at 510°C, and finishes at 690°C, with the endothermic peak of 624°C. The

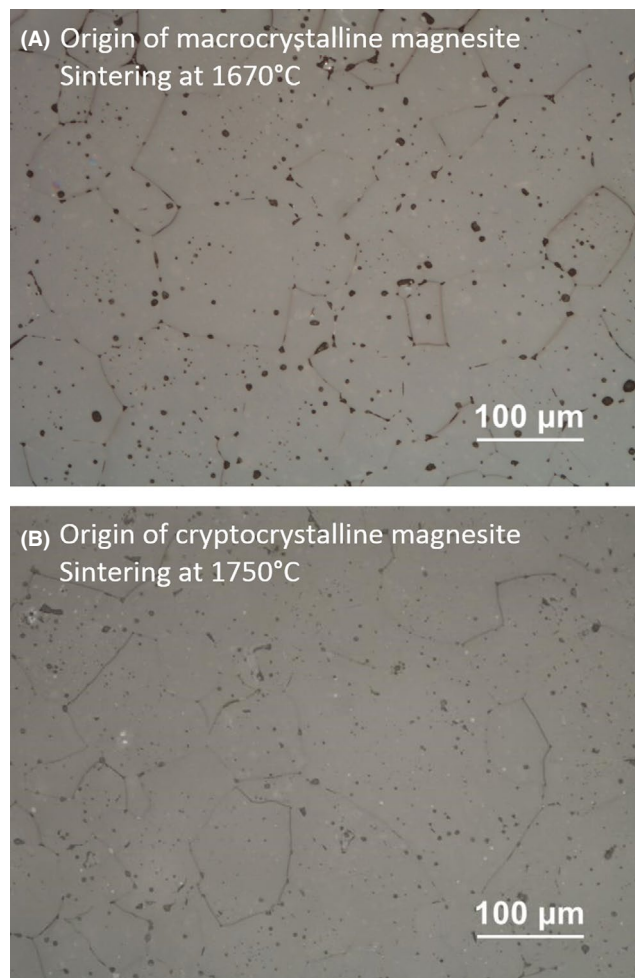


**FIGURE 10** Microstructures of high-purity, dense sintered magnesia

macrocrystalline magnesite exhibits the endothermic reaction for decomposition at the temperatures between 512 and 712°C, being most drastic at 652°C as the endothermic peak.

2. Significant differences of activity for the caustic magnesia obtained by calcining at different temperatures exist. The highest activity occurs at 700°C for the cryptocrystalline magnesite and at 800°C for the macrocrystalline one.
3. With a two-step sintering process, the highest bulk density of magnesia attainable is 3.26 g/cm<sup>3</sup> from the cryptocrystalline magnesite and only 3.14 g/cm<sup>3</sup> from the macrocrystalline magnesite.

4. With a three-step sintering process, the highest bulk density obtainable is  $3.48 \text{ g/cm}^3$ , starting with a cryptocrystalline Tibetan magnesite, after sintering at  $1750^\circ\text{C}$  while it only reach  $3.47 \text{ g/cm}^3$ , starting with a macrocrystalline Liaoning magnesite and sintering at  $1670^\circ\text{C}$ .
5. In order to reach such performance it is essential to recalcine the magnesium hydroxide powder at  $1000^\circ\text{C}$  for both types, after due milling and compacting prior to sintering.

## ORCID

Zongqi Guo  <https://orcid.org/0000-0002-5321-2133>

## REFERENCES

1. Bhatti AS, Dollimore D, Dyer A. Magnesite from seawater: a review. *Clay Miner.* 1984;19(5):865–75.
2. Rong ZH, Liang XY, Feng SC. Development of the technology for producing high-quality magnesia from Haichengmagnesite, China. *Proceedings of International Symposium on Refractories*; 1988 Nov 15–18; Hangzhou, China. p. 179–88.
3. He ZY, Ma LT, Liu BK. Crystallographic characterization and thermal decomposition behavior of high purity microcrystalline magnesite. *Proceedings of UNITECR2011*; 2011 Oct 30–Nov 2; Kyoto, Japan. p. 2-B2-16.
4. Feng RT, Liu BK, Tian XL. Research and application of microcrystalline magnesite in Tibet, China. *Proceedings of UNITECR2019*; 2019 Oct 13–16; Yokohama, Japan. p. 15-B-15.
5. Rao DS, Geng XM, Xu XW. Characters and sintering of magnesite in the south of Liaoning province. *Proceedings of International Symposium on Refractories*; 1988 Nov 15–18; Hangzhou, China. p. 217–23.
6. Li N, Chen RR. Kinetics of sintering and grain growth of MgO during calcination of magnesite. *J Chin Ceram Soc.* 1989;17(1):64–8.
7. Zhou BY, Li ZJ, Wu F. Periclase particles densification behavior at early stage of block magnesite sintering. *Trans Mater Heat Treat.* 2015;36(5):1–4.
8. Kim MG, Dahmen U, Searcy AW. Structural transformations in the decomposition of  $\text{Mg}(\text{OH})_2$  and  $\text{MgCO}_3$ . *J Am Ceram Soc.* 1987;70(3):146–54.
9. Yu JK, Ma PC, Li H, Yuan L. Preparation of high-density magnesia from natural magnesite. *Proceedings of UNITECR2011*; 2011 Oct 30–Nov 2; Kyoto, Japan. p. 31-E-10.
10. Livey DT, Wanklyn BM, Hewitt M, Murray P. The properties of MgO powders prepared by the decomposition of  $\text{Mg}(\text{OH})_2$ . *Trans Br Ceram Soc.* 1957;56(5):217–36.
11. Yu GC. The divacancies in MgO — II. the solid solution ( $\text{MgO}$ ,  $\text{H}_2\text{O}$ ). *J Chin Ceram Soc.* 1978;6(4):251–5.

**How to cite this article:** Guo Z, Ma Y, Rigaud M. Sinterability of macrocrystalline and cryptocrystalline magnesite to refractory magnesia. *Int J Ceramic Eng Sci.* 2020;2:303–309. <https://doi.org/10.1002/ces2.10068>